TECHNICAL UNIVERSITY OF CLUJ-NAPOCA

ACTA TECHNICA NAPOCENSIS

Series: Applied Mathematics, Mechanics, and Engineering
Vol. 69, Issue II, June, 2026

STUDY OF THE MECHANICAL BEHAVIOR OF RUȘCHIȚA MARBLE THROUGH EXPERIMENTAL TESTING AND FDEM SIMULATION

Andrei ANDRAS

Abstract: *This study examines the mechanical behavior and failure of Rușchița marble using a combined experimental and numerical approach. Uniaxial compressive strength tests were performed on dry and water-saturated core specimens to evaluate the effect of moisture on strength and stiffness. Dry samples showed higher compressive strength, while saturated samples exhibited reduced mechanical performance due to water-weakening effects. To examine fracture development, a two-dimensional finite-discrete element method model was developed in Irazu. The simulation reproduced the main stages of brittle failure, including damage localization, crack initiation, crack propagation, and fragment detachment. Good qualitative agreement was observed between the simulated fracture pattern and the laboratory failure mode, confirming the usefulness of the combined method for assessing marble behavior.*
Keywords: *marble; mechanical behavior; uniaxial compressive strength; finite–discrete element method; brittle failure; fracture propagation*

1. INTRODUCTION

Carbonate rocks are sedimentary rocks mainly composed of calcite and dolomite, formed through biological accumulation and chemical precipitation in marine environments. Overall, they are an essential natural resource with diverse applications ranging from heavy industry to art and design.

Limestone and marble represent two key forms of carbonate rocks with different origins and properties. Limestone is a sedimentary rock widely used in construction, cement production, and various industries, while marble forms when limestone undergoes metamorphism, resulting in a denser and more durable material. Due to its strength and aesthetic qualities, marble is highly valued in architecture and decorative applications. [1-3].

The physical and mechanical properties of carbonate rocks—such as density, porosity, and compressive strength—are essential for determining their behavior in engineering and environmental conditions.

These properties influence stability, durability, and resistance to weathering, and can vary significantly depending on factors like water content and internal structure [4]. Because carbonate rocks are often heterogeneous [5], in order to avoid structural or geotechnical failures, a very accurate characterization is always necessary [6].

These characteristics are usually determined using laboratory tests and analytical methods, such as unconfined compressive strength testing, petrographic analysis, and advanced imaging techniques [7-10].

While laboratory data provide precise measurements, numerical modelling methods like FDEM [11] simulate large-scale behavior and fracture processes.

The integration of both approaches ensures a more complete and reliable understanding of carbonate rock performance in engineering and geological applications [12-16].

Thus, this study presents the results obtained for Romanian carbonate rocks like Ruschița marble that was subjected to such a combined experimental and numerical modelling, using laboratory testing and Geomechanica Irazu commercial software.

Received: 05.04.26; **Similaritie**s: 12.05.26: **Reviewed**:18.05. /19.05.26: **Accepted** 04.06.26.

2. METHODOLOGY

The marble was collected from Rușchița quarry (Romania) in form of rectangular blocks (Figure 1). In order to mitigate measurement errors associated with anisotropy, the sampling prioritized the collection of block samples without visible bedding planes.

Fig. 1. Rectangular blocks of marble samples

These blocks were transported to the laboratory in order to core the samples. A number of 30 cylindrical core samples were prepared (Figure 2) according to the ASTM Standards, having approximately 2:1 length to diameter ratio. [17, 18].

Fig. 2. Cored samples of marble

The best 20 cores were selected and all their ends were ground to have parallel and smooth surfaces normal to the long axis. According to the standard, the sample ends must be flat within 0.02 mm and perpendicular to the axis within 0.06 degrees.

Before testing, all the samples were conditioned by drying in an oven for 48 hours in order to remove all initial moisture (Figure 3), and after cooling to room temperature, the dry weight along with length and diameter were measured (Figure 4).

Fig. 3. Drying of **c**ore samples

Fig. 4. Measuring and weighing of **c**ore samples

In order to obtain the mechanical properties in water-saturated conditions, which often reduce the marble compressive strength compared to dry conditions, half of the samples were saturated using the immersion soaking method, by submerging them in water at 20°C for 15 hours, then the constant saturated mass was measured (Figure 5).

Fig. 5. Saturation of **c**ore samples

3. EXPERIMENTAL TESTING

Uniaxial Compressive Strength (UCS) testing is a standard way to quantify the maximum axial load a rock can withstand without lateral confinement before its failure.

The test involves a constant compressive force applied to the cylindrical sample prepared according to the standards as described in section 2, until it fails. For accurate results several samples are prepared and tested.

The loading apparatus is a hydraulic press, where the specimen is secured between a set of steel platens, with a small axial load (around 100 N) applied to secure it.

A hydraulic cylinder then applies a constant rate of strain (typically between 0.5% to 2% of the sample height per minute) until the specimen fails by cracking or significant deformation.

Figures 6a shows one sample of marble during the securing phase, while figure 6b shows the failed sample at the end of the test.

a **b**

Fig.6. One sample of marble
a) during securing; b) failed at the end of the test.

The axial strain (ε_a) in the case of UCS testing represents the deformation of the rock sample along the vertical axis:

$$\varepsilon_a = \frac{\Delta l}{L_0} \quad [\%] \qquad (1)$$

It is measured as percentage or ratio of length change (Δl) compared to initial specimen length (L_0), and it quantifies how much the material compresses longitudinally as vertical load is applied on it under unconfined conditions.

The peak load at failure is recorded and used to calculate UCS. The fundamental equation for UCS noted with σ_{UCS} is

$$\sigma_{UCS} = \frac{P_{\max}}{A_0} \quad [\text{MPa}] \qquad (2)$$

where $P_{\max}$ is the maximum axial load recorded by the testing machine at the point of failure, and A_0 is the area of the cross section of the sample.

The two data recorded during the test are used to plot the stress-strain curve allowing to visualize the material behavior.

From the experimentally determined data, Young modulus (E) can be calculated:

$$E = \frac{\Delta\sigma}{\Delta\varepsilon_a} \quad [\text{GPa}] \qquad (3)$$

It represents the ratio between the axial stress and strain, and is normally calculated at a stress-strain level of about 50% of the maximum load.

4. RESULTS AND DISCUSSION OF UCS TESTING

The tests were conducted in two batches of five dry and five saturated specimens. Figure 7 shows the failed samples in the first batch.

Fig.7. Failed samples in test batch 1.

The initial diameter, length, and mass for each cored sample that was prepared according to the standards from section 2, as well as the calculated cross-section area, the load force applied by the press, and the uniaxial compressive stress results obtained after testing, are summarized in table 1.

It is important to mention that the testing of the saturated samples was performed immediately after removal from water, in order to avoid partial drying that could influence the results.

The values obtained for the UCS for each sample in table 1 are represented in figure 8.

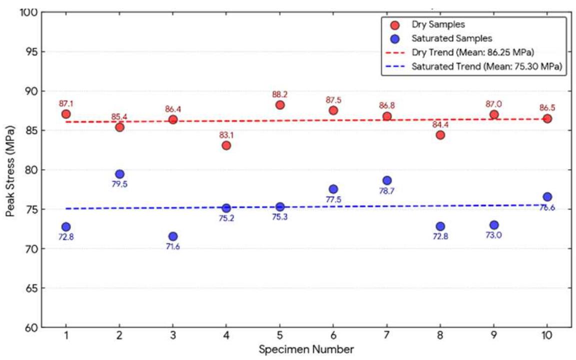

Fig.8. UCS Values and linear trends for marble samples

This scatter plot illustrates the UCS for 10 dry and 10 saturated marble specimens and shows a distinct performance gap between the two states. The dry samples (red) exhibit a high level of structural integrity, with individual peak stress values ranging from 83.09 to 88.23 MPa and a mean UCS of 86.25 MPa. The saturated samples (blue) showed a decline in strength, with values falling between 71.56 and 79.47 MPa, resulting in a significantly lower mean UCS of 75.30 MPa.

A comparative analysis reveals a clear and consistent strength reduction in the saturated specimens, which averaged 10.95 MPa (12.7%) lower than their dry counterparts. This phenomenon, often attributed to the reduction of internal friction and grain-boundary weakening caused by moisture, is underscored by the relatively flat linear trendlines for both datasets. The stability of these trends suggests high sample uniformity and consistent experimental conditions across all 20 tests, aligning with established rock mechanics observations regarding water-weakening effects in carbonate rocks [19].

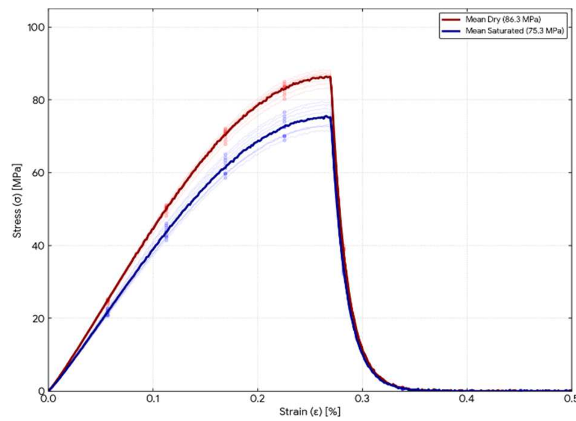

Fig.9. Uniaxial Stress-Strain curves

Figure 9 is the uniaxial stress-strain diagram, illustrating the mechanical behavior of the 20 marble samples under dry and saturated conditions. Individual samples are represented by thin lines and markers (red circles for dry, blue squares for saturated) to highlight the experimental spread. The bold curves represent the mean response.

Table 1. Dimensional and weight of samples, calculated area and stress results measured

Dry Sample	Diam. [cm]	L_0 [cm]	F [kN]	A_0	σ_{UCS}	Saturated Sample	Diam. [cm]	L_0 [cm]	F [kN]	A_0	σ_{UCS}
DM1	5.312	10.847	193.000	22.162	87.0866	**SM1**	5.307	10.782	161.000	22.120	72.7843
DM2	5.294	11.019	188.000	22.012	85.4083	**SM2**	5.295	10.765	175.000	22.020	79.4724
DM3	5.292	10.875	190.000	21.995	86.3822	**SM3**	5.302	10.948	158.000	22.078	71.5629
DM4	5.281	10.875	182.000	21.904	83.0901	**SM4**	5.303	10.783	166.000	22.087	75.1580
DM5	5.298	10.883	194.500	22.045	88.2279	**SM5**	5.249	10.926	163.000	21.639	75.3259
DM6	5.305	11.002	193.500	22.103	87.5428	**SM6**	5.294	11.019	175.000	22.012	77.5489
DM7	5.279	10.998	190.000	21.887	86.8081	**SM7**	5.288	11.020	168.500	21.962	78.6518
DM8	5.282	10.879	185.000	21.912	84.4277	**SM8**	5.298	10.875	177.500	22.045	72.8478
DM9	5.307	11.020	192.500	22.120	87.0247	**SM9**	5.294	11.002	173.000	22.012	73.0248
DM10	5.288	11.010	190.000	21.962	86.5129	**SM10**	5.311	10.883	168.500	22.154	76.5748

Results show a classic brittle response. There is very little plastic deformation (yielding) before the peak, followed by a catastrophic stress drop. This indicates that the marble specimens failed by sudden macro-cracking or axial splitting.

The saturated samples (blue) consistently peak lower than dry samples (red). This "water-weakening" effect is likely due to the reduction of surface energy on micro-cracks and the lubrication of grain boundaries, which lowers internal friction. At a constant strain rate of 0.5% length/min., the failure occurred around 32.5 seconds, and the calculated failure strain is 0.27%. Based on the "stiffness" of the rock visualized at the linear elastic region of the stress-strain curves, considering the UCS data (mean), and the 32.5-second failure time, the Young's Modulus was determined:

$$E_{DRY} \approx \frac{86.3\,\text{MPa}}{0.0027} = 31.9\,\text{GPa}$$
$$E_{SATURATED} \approx \frac{75.3\text{MPa}}{0.0027} = 27.9\,\text{GPa} \quad (4)$$

These values suggests that saturation doesn't just lower the strength, but also the stiffness. The saturated marble is roughly 12.5% less stiff than the dry one. A Young's Modulus of ~32GPa is common in literature for many commercial marbles (which range from 20 to 70 GPa).

From a mechanical behavior and fracture analysis point of view, the stress-strain curves provide a clear roadmap of the internal damage and eventual fracture of the rock mass. In rock mechanics, the curve is typically divided into four distinct regions, each corresponding to a physical change in the marble:

Region I - Crack closure: At the very start of the curves (concave segment at 0% to ~0.05% strain), the slight upward scoop represents the closure of pre-existing micro-fissures and pores within the marble. This is a non-linear phase in which the specimen adjusts to the applied load and becomes more compact

Region II - Linear Elastic Phase: This is the long, straight part of the curve where the marble stores energy. This slope defines the Young's Modulus. In this phase, the mineral grains are deforming without permanent damage, the sample would return to its original height if the load would stop acting on it.

Region III - Crack Initiation and Yielding: As the curve starts to bend (near the peak at ~0.2% strain), the marble reaches its elastic limit. Stable micro-cracking begins, usually starting at grain boundaries. The visible yielding that can be seen—the rounding of the top—indicates that these micro-cracks are starting to coalesce, turning the rock from a solid block into a failing structure.

Region IV - Failure and Brittle Drop: Once the peak UCS is reached, the marble undergoes unstable crack propagation. The sharp drop in stress is characteristic of brittle fracture. In marble, this manifests as axial splitting with vertical cracks parallel to the load and shear failure with a diagonal fracture plane.

The saturated curves show a lower peak and a slightly less steep linear region. In rock mechanics terms, water saturation lowers the fracture toughness. Water molecules penetrate the micro-cracks during the yielding phase, increasing pore pressure and lubricating grain contacts. This causes the transition from Region II to Region III to happen much earlier, thus the 12.7% strength reduction observed in the tested samples. Considering the findings, the analyzed marble acts as a high-quality dense metamorphic brittle rock, with a sudden and energy-releasing failure.

5. NUMERICAL SIMULATION

For a more in-depth analysis and in order to clarify some aspects of the mechanical properties and failure patterns of marble, finite–discrete element method (FDEM) was selected to simulate the UCS tests using the commercial software Irazu 2D version 6.2.

FDEM is a numerical approach that combines continuum mechanics with discontinuum behavior [20], allowing rock to deform as a continuous material at first and then naturally fracture, separate, and form blocks as damage progresses. In rock mechanics it is useful for simulating crack initiation, propagation, coalescence, and post-peak brittle failure under tests such as uniaxial compression, Brazilian tension, or notched fracture experiments, where

FEM often struggles to capture the full transition from intact rock to fragmented material [21,22].

The simulation workflow comprised the following steps, as shown in figures 10-13:

(1) Construction of the geometric model of the steel platens (top and bottom) and the marble sample (with real dimensions of 50 mm width x100 mm height);

(2) Naming of model parts and definition of material properties for each of the models;

(3) Application of boundary conditions for the platens and marble sample and meshing setup;

(4) Definition of the run options (the vertical speed of the platens, the number of time steps, time step size) for the simulation.

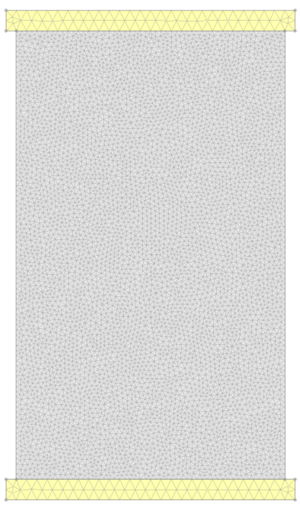

Fig. 10. Geometric model of platens/sample

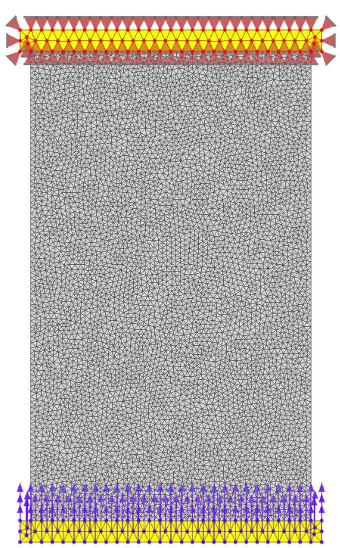

Fig. 11. Meshing and boundary conditions

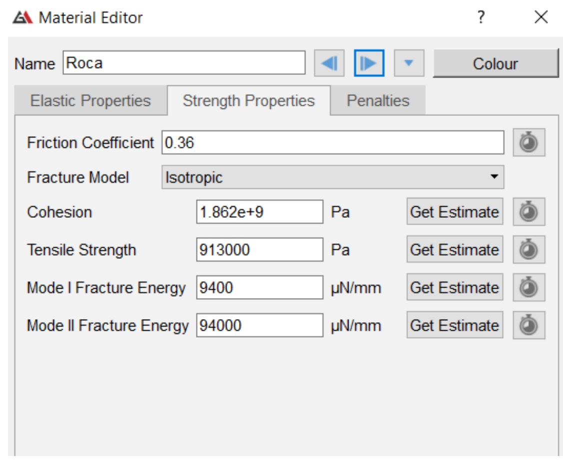

Fig. 12. Material properties definition

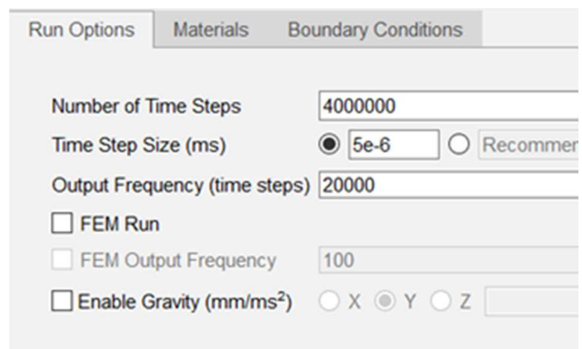

Fig. 13. Run options for simulation

One important aspect to consider is that even though Irazu makes use of high-performance GPU acceleration parallel computing, being 15 to 100 times faster than CPU only performance, this kind of simulation is still a high computational demanding task, influenced by the available hardware. On the i7/GeForce RTX 3080Ti configuration used, the actual run time was several hours. Because of this limitation, the simulation was run only for the saturated sample.

After the setup is finished, simulation is run and two types of results are obtained:

A). First, there are numerical values for a wide range of data like: mean stress magnitude; principal deviatoric stress max; principal deviatoric stress min; principal strains max; principal strains min; principal stresses max; principal stresses min; volumetric strain magnitude; - stress magnitudes; stresses on xx, xy, yx and yy direction.

All data can be exported as .csv files for further analysis or used directly within the Irazu software to generate plots.

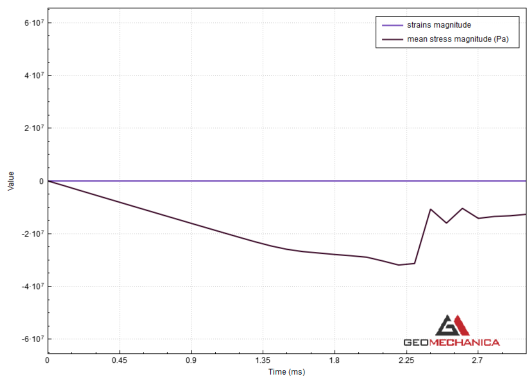

Fig. 14. Mean stress magnitude

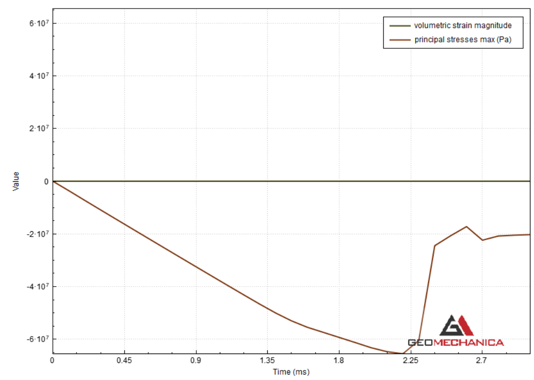

Fig 15. Principal stresses max

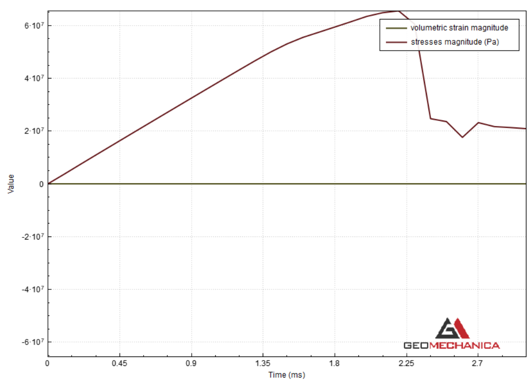

Fig. 16. Stresses magnitude

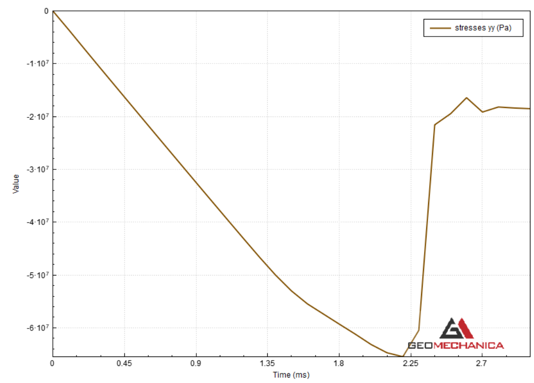

Fig. 17. Stresses on yy direction

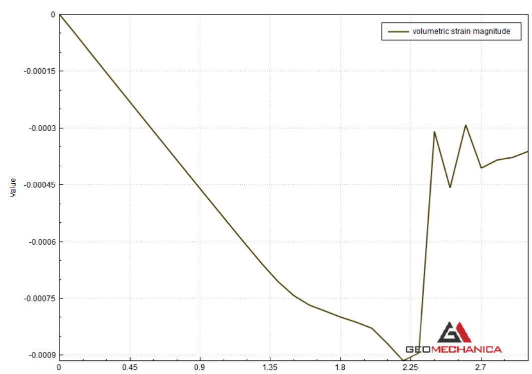

Fig. 18. Volumetric strain magnitude

The Irazu plots in figures 14-18 indicate the typical brittle response of marble under uniaxial compression.

Stress increases almost linearly up to about 2.2–2.3 ms, reaching a peak close to 65 MPa, which marks the maximum load-bearing capacity of the sample. Immediately after this point, both the overall stress and the axial stress in the loading direction show a sharp drop, indicating sudden failure and rapid crack propagation. The fact that stress does not fall to zero after peak suggests that the broken specimen still carries some residual load through fragment contact and friction along the newly formed fracture surfaces. At the same time, the volumetric strain becomes progressively more negative during loading, showing that the sample is compacting as pores and microcracks close. Just before failure, it reaches its maximum compaction, then abruptly shifts toward less negative values and begins to fluctuate. This reflects the transition from compaction to dilation caused by macrocrack formation, fragment detachment, and post-failure rearrangement.

B). The second type of output is the visual representation of actual cracking and failure. The FDEM sequence shown in figure 19, clearly shows the full failure evolution of the Rușchița marble sample.

The geomechanics interpretation of the sequence is:

At the beginning of the test, from 0 to about 0.9 ms, the marble sample behaves essentially elastically, with very low and fairly uniform displacement across the specimen and no visible localization of damage.

As loading continues toward roughly 1.5 ms, a subtle displacement gradient begins to develop, marking the transition from purely elastic response to the onset of microcrack nucleation.

Between about 1.5 and 2.1 ms, this localized behavior becomes more evident: deformation begins to localize into inclined bands, suggesting the onset of internal damage and stress concentration. This stage corresponds to the pre-peak damage regime, when the rock is still carrying increasing load but is already preparing for unstable failure.

Around 2.3 ms, the specimen reaches peak strength and the first clear macrocrack appears, initiating near the central-right zone while another crack starts near the upper-right edge.

From 2.4 to 2.7 ms, these cracks propagate rapidly and connect with a major diagonal fracture rising from the lower-left part of the sample, showing unstable crack growth after peak strength, which is characteristic of brittle shear-dominated failure.

From 2.7 to 3.0 ms, the fracture network becomes fully developed. A dominant inclined crack crosses the specimen, secondary branches form, and a damaged zone opens on the right side, where a fragment begins to detach. This is typical of brittle, shear-dominated failure with mixed tensile-shear cracking.

The final image in the sequence is the laboratory sample, which shows a very similar macroscopic failure pattern: a main inclined rupture surface with branching cracks and separation of a side fragment. That suggests the numerical model reproduces the real failure mode reasonably well, especially in terms of crack orientation, localization, and final fragmentation.

The model indicates a typical brittle response of marble under uniaxial compression, characterized by a clear elastic phase, a short damage-development stage, a sharp peak stress, and a sudden post-peak drop. Failure is dominated by diagonal shear with mixed tensile-

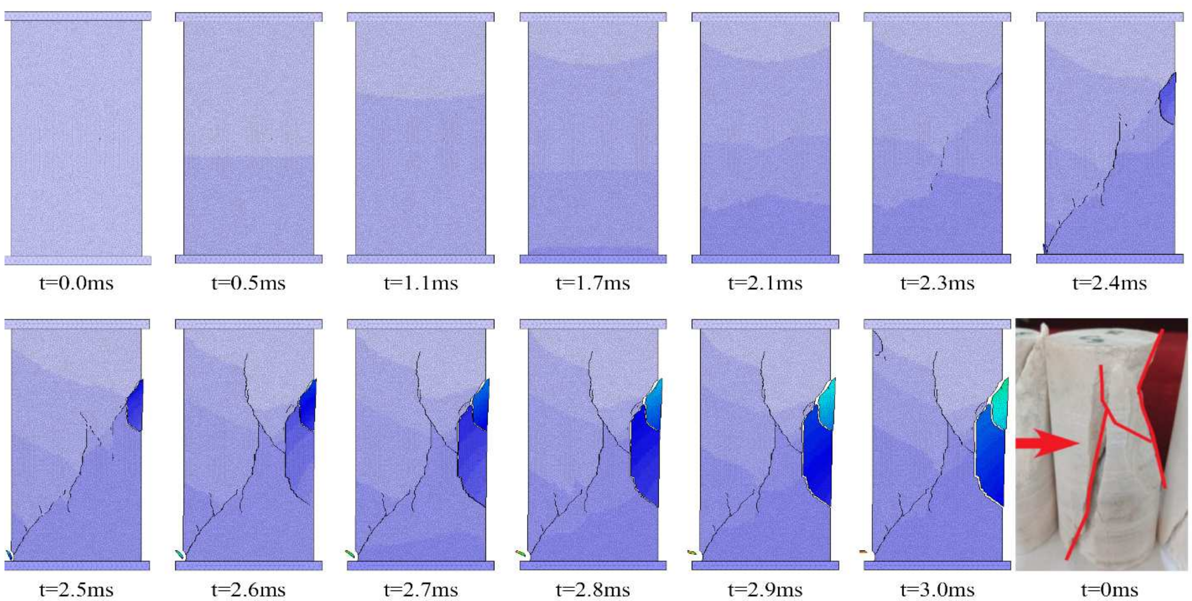

Fig. 19. Visual representation of FDEM simulation timestamped sequence of sample failure

shear cracking, showing that rupture is controlled by strain localization within a narrow band rather than by diffuse crushing.

The simulation also captures the transition from continuum deformation to discontinuum fracture, highlighting the ability of FDEM to reproduce the expected behavior of marble: high initial stiffness, limited inelastic deformation before peak, and abrupt collapse after the formation of a critical crack network. Overall, the numerical results are consistent with the fracture sequence observed in the simulation images.

6. CONCLUSION

The UCS tests showed that dry Rușchița marble specimens had consistently higher strength than water-saturated specimens, confirming the weakening effect of moisture on the tested carbonate rock. On average, the saturated samples exhibited a compressive strength reduction of about 10.95 MPa, corresponding to approximately 12.7% compared with the dry samples.

The experimental stress-strain curves indicated a predominantly brittle mechanical response, characterized by a short inelastic stage, peak strength, and a sudden post-peak stress drop. In addition to reducing strength, saturation also led to a decrease in stiffness.

The FDEM simulation reproduced the main stages of failure, including damage localization, crack initiation, crack propagation, and fragment detachment. The final fracture geometry showed good qualitative agreement with the laboratory specimen, particularly in terms of crack inclination, branching, and local fragment separation.

Overall, the coupled experimental-numerical approach proved effective for assessing the mechanical response and failure mechanisms of marble. However, since the numerical analysis was performed only for the saturated specimen, this should be considered a limitation of the present study. Even so, the proposed methodology can be extended to other carbonate rocks used in engineering applications.

7. REFERENCES

[1] Haqbin, M., Inanch, S., Qarizada, K., Qarizada, D. Unveiling the geological significance and industrial application of limestone: A comprehensive review. *IEM Journal* **2024**, *85(1)*, 31-43.

[2] Zhang, T. Geological and geochemical characteristics and genesis of carbonate rocks in a certain area. *E3S Web Conf.* **2022**, *358*, 02034.

[3] Coli, M., Criscuolo, A. The Carrara marble: geology, geomechanics and quarrying. *IOP Conf. Ser. Earth Environ. Sci.* **2021**, *833*(1), 012120.

[4] Abd El Aal, A., Abdullah, G.M.S., Radwan, A.E., Ali, S.H., Wahid, A., Shoukat, N., Zakhera, M., Moftah, H. Experimental study of the influence of the degree of saturation on physical and mechanical properties of carbonate rocks in the Jurassic Tuwaiq Mountain Formation (Saudi Arabia). *Geol. J.* **2023**, *58*(11), 3970-3980.

[5] Regnet, J.B., David, C., Robion, P., Menéndez, B. Microstructures and physical properties in carbonate rocks: A comprehensive review. *Mar. Pet. Geol.* **2019**, *103*, 366-376.

[6] Arman, H., Hussein, S., Alshehyari, S.K., El Imam, H.H., Asmaa, A.A., Albedwawi, M.A. Likely effects of geological features on carbonate rock strength. *Rev. Environ. Earth Sci.* **2018**, *5*(1), 1-7.

[7] Demirdag, S., Tufekci, K., Kayacan, R., Yavuz, H., Altindag, R. Dynamic mechanical behavior of some carbonate rocks. *Int. J. Rock Mech. Min. Sci.* **2010**, *47*(2), 307-312.

[8] Alomari, E., Ng, K., Khatri, L. Experimental investigation and prediction of mechanical properties of carbonate rocks under uniaxial and triaxial compressions. *Materials* **2025**, *18*, 1211.

[9] Sadeghi, E., Nikudel, M.R., Khamehchiyan, M., Kavussi, A. Estimation of unconfined compressive strength (UCS) of carbonate rocks by index mechanical tests and specimen size properties: Central Alborz Zone of Iran. *Rock Mech. Rock Eng.* **2022**, *55*(1), 125-145.

[10] Kallimogiannis, V., Saroglou, C.

Mechanical properties of carbonate fault rocks. *Int. J. Rock Mech. Min. Sci.* **2024**, *176*, 105681.
[11] Lisjak, A., Kaifosh, P., He, L., Tatone, B.S.A., Mahabadi, O.K., Grasselli, G. A 2D, fully coupled, hydro-mechanical, FDEM formulation for modelling fracturing processes in discontinuous, porous rock masses. *Comput. Geotech.* **2017**, *81*, 1-18.
[12] Enbing, Y. FDEM numerical simulation of size effect on mechanical properties of basalts with hidden microcracks. *Sci. Rep.* **2025**, *15*, 7246.
[13] Hamdi, P., Stead, D., Elmo, D. Characterizing the influence of stress-induced microcracks on the laboratory strength and fracture development in brittle rocks using a finite-discrete element method-micro discrete fracture network (FDEM-μDFN) approach. *J. Rock Mech. Geotech. Eng.* **2015**, *7*(6), 609-625.
[14] Hu, L., Wang, F., Jiang, F., Huang, G. Study on the influence of mineral composition on the mechanical properties of granite based on FDEM-GBM method. *Simul. Model. Pract. Theory* **2023**, *129*, 102834.
[15] Popescu, F.D., Andras, A., Radu, S.M., Brinas, I., Iladie, C.-M. Numerical investigation of the slope stability in the waste dumps of Romanian lignite open-pit mines using the shear strength reduction method. *Appl. Sci.* **2024**, *14*, 9875.
[16] Pasculescu, D.; Niculescu, T. Study of transient inductive-capacitive circuits using data acquisition systems, **2015**. *Int. Multidiscip. Sci. GeoConf. SGEM* **2015**, *2*(1), 323-329.
[17] ASTM D2938-95. *Standard Test Method for Unconfined Compressive Strength of Intact Rock Core Specimens*; ASTM International: West Conshohocken, PA, USA, 1995.
[18] ASTM D7012-14e1. *Standard Test Methods for Compressive Strength and Elastic Moduli of Intact Rock Core Specimens under Varying States of Stress and Temperatures*; ASTM International: West Conshohocken, PA, USA, 2014.
[19] Romana, M., Vásárhelyi, B. A discussion on the decrease of unconfined compressive strength between saturated and dry rock samples. In *Proc. 11th ISRM Congress*; 2007.
[20] Munjiza, A. *The Combined Finite-Discrete Element Method*; John Wiley & Sons: Chichester, UK, 2004.
[21] An, H., Wu, S., Liu, H., Wang, X. Hybrid finite-discrete element modelling of various rock fracture modes during three conventional bending tests. *Sustainability* **2022**, *14*, 592.
[22] Song, Y., Fan, Y., An, H., Liu, H., Wu, S. Investigation of the dynamic pure-mode-II fracture initiation and propagation of rock during four-point bending test using hybrid finite-discrete element method. *Sustainability* **2022**, *14*, 10200.

Studiul comportamentului mecanic al marmurei de rușchița prin testare experimentală și simulare FDEM

Rezumat: Acest studiu analizează comportamentul mecanic și cedarea marmurei de Rușchița printr-o abordare experimentală și numerică combinată. Au fost efectuate încercări de compresiune uniaxială pe carote uscate și saturate cu apă pentru a evalua efectul umidității asupra rezistenței și rigidității. Probele uscate au prezentat rezistențe mai mari, în timp ce probele saturate au evidențiat o reducere a performanței mecanice. Pentru analiza dezvoltării fracturilor, a fost realizat în Irazu un model bidimensional bazat pe metoda elementelor finite–discrete. Simularea a reprodus principalele etape ale cedării fragile, de la localizarea degradării și inițierea fisurilor până la propagarea acestora și desprinderea fragmentelor. S-a observat o bună concordanță calitativă între tiparul de fracturare simulat și modul de cedare observat în laborator, confirmând utilitatea metodei combinate pentru evaluarea comportamentului marmurei.

Cuvinte-cheie: marmură; comportament mecanic; rezistență la compresiune uniaxială; metoda elementelor finite–discrete; cedare fragilă; propagarea fisurilor

Andrei ANDRAȘ, PhD Eng. Habil, Professor., University of Petroșani, Department of Mechanical, Industrial and Transport Engineering, andrei.andras@gmail.com, 0722366653.